



## Left perirhinal cortex codes for semantic similarity between written words defined from cued word association

Antonietta Gabriella Liuzzi<sup>a</sup>, Patrick Dupont<sup>a</sup>, Ronald Peeters<sup>c</sup>, Rose Bruffaerts<sup>a,b</sup>, Simon De Deyne<sup>d</sup>, Gert Storms<sup>d</sup>, Rik Vandenberghe<sup>a,b,\*</sup>

<sup>a</sup> Laboratory for Cognitive Neurology, Department of Neurosciences, KU Leuven, Belgium

<sup>b</sup> Neurology Department, University Hospitals Leuven, 3000, Leuven, Belgium

<sup>c</sup> Radiology Department, University Hospitals Leuven, 3000, Leuven, Belgium

<sup>d</sup> Laboratory of Experimental Psychology, Humanities and Social Sciences Group, KU Leuven, Belgium

### A B S T R A C T

Knowledge of visual and nonvisual attributes of concrete entities is distributed over neocortical uni- and polymodal association cortex. Here we investigated the role of left perirhinal cortex in explicit knowledge retrieval from written words. We examined whether it extended across visual and nonvisual properties, animate and inanimate entities, how this differed from picture input and how specific it was for perirhinal cortex compared to surrounding structures. The semantic similarity between stimuli was determined on the basis of a word association-based model. Eighteen participants participated in this event-related fMRI experiment. During property verification, the left perirhinal cortex coded for the similarity in meaning between written words. No differences were found between visual and nonvisual properties or between animate and inanimate entities. Among the surrounding regions, a semantic similarity effect for written words was also present in the left parahippocampal gyrus, but not in the hippocampus nor in the right perirhinal cortex. Univariate analysis revealed higher activity for visual property verification in visual processing regions and for nonvisual property verification in an extended system encompassing the superior temporal sulcus along its anterior-posterior axis, the inferior and the superior frontal gyrus. The association strength between the concept and the property correlated positively with fMRI response amplitude in visual processing regions, and negatively with response amplitude in left inferior and superior frontal gyrus. The current findings establish that input-modality determines the semantic similarity effect in left perirhinal cortex more than the content of the knowledge retrieved or the semantic control demand do. We propose that left perirhinal cortex codes for the association between a concrete written word and the object it refers to and operates as a connector hub linking written word input to the distributed cortical representation of word meaning.

### 1. Introduction

The representation of knowledge in the human brain is a central topic in cognitive neuroscience. There currently is a general consensus that knowledge of concrete entities is represented in a distributed manner over the neocortex (Binder et al., 2016; Huth et al., 2016; Lambon-Ralph et al., 2016). This representation partly overlaps with the unimodal regions mediating the perception of these objects (Chao et al., 1999; Vandenberghe et al., 2006; Martin, 2007; Fernandino et al., 2015a,b; Huth et al., 2016; Binder et al., 2016), and partly with heteromodal convergence zones (Huth et al., 2016; Fernandino et al., 2015a,b, 2016).

The points of entry and the stages through which different input modalities access the distributed representations of meaning have been researched intensively. Recently we examined using fMRI and a property verification task where the semantic similarity is represented for written words specifically (Bruffaerts et al., 2013; Liuzzi et al., 2015, 2017): During property verification the semantic similarity between the probe

nouns was represented by the activity patterns in left perirhinal cortex. No such effect was seen for auditory words or pictures (Bruffaerts et al., 2013; Liuzzi et al., 2015, 2017). The semantic similarity effect for written nouns was independently replicated by another centre also using property verification as a task (Martin et al., 2018).

This consistent finding can be interpreted in several ways: Because the experiments were done with animate entities and mainly with visual properties, involvement of left perirhinal cortex could relate to the visual nature of the knowledge to be retrieved given the position of left perirhinal cortex at the apex of the ventral occipitotemporal processing stream. This hypothesis would predict that the effect would be stronger for visual than for nonvisual properties. It may also predict a stronger semantic similarity effect for animate than for inanimate entities: Animate entities are often considered to be more heavily weighted towards sensory (particularly visual) attributes compared to functional-associative attributes than inanimate entities (Farah and McClelland, 1991). This distinction may not be valid for all entities within these two

\* Corresponding author. Neurology Department, University Hospitals Leuven, Herestraat 49 bus 7003, B-3000, Leuven, Belgium.

E-mail address: [rik.vandenberghe@uzleuven.be](mailto:rik.vandenberghe@uzleuven.be) (R. Vandenberghe).

<https://doi.org/10.1016/j.neuroimage.2019.02.011>

Received 20 September 2018; Received in revised form 31 January 2019; Accepted 5 February 2019

Available online 10 February 2019

1053-8119/© 2019 The Authors. Published by Elsevier Inc. This is an open access article under the CC BY-NC-ND license (<http://creativecommons.org/licenses/by-nc-nd/4.0/>).

broad categories. In the current experiment the subset of inanimate entities was restricted to manipulable entities. Lesions of the ventral occipitotemporal pathway may give rise to category-specific effects where processing of animate entities is more affected than inanimate entities (for review see Gainotti (2000)). Hence the hypothesis that the perirhinal effect could have been stronger for animate than for inanimate entities. The hypothesis may also explain why the semantic similarity effect was weaker for picture input: Visual properties may be retrieved for pictures at the earlier, structural description stage (Humphreys and Forde, 2001). Accordingly, the involvement of the left perirhinal cortex in the semantic processing of written words and pictures (Bright et al., 2004; Liu et al., 2009; Peelen and Caramazza, 2012; Fairhall and Caramazza, 2013) may depend on the type of information that has to be retrieved. Alternatively, the perirhinal involvement may relate to the visual nature of written words regardless of stimulus category or type of task-related retrieval. This would explain why no semantic similarity effect was seen for auditory words. In these experiments (Liuzzi et al., 2017) a semantic similarity effect for auditory words was seen in the anterior third of the superior temporal sulcus at a distance from the visual occipitotemporal processing stream. A crossmodal semantic similarity effect for both written and auditory words was seen in the left pars triangularis, a common projection zone for both left perirhinal and left anterolateral temporal cortex (Liuzzi et al., 2017).

The current experiment aimed to evaluate these two possibilities. We examined whether the semantic similarity effect for written nouns could be replicated when a wider range of categories, both animate and inanimate, was used as well as for a wider range of properties, both visual and nonvisual properties. The experiment aimed to examine whether the specificity for written nouns compared to pictures was maintained under these circumstances. In the current experiment visual properties refer to properties such as colour, shape, size and parts of objects. Non-visual properties may be non-physical and abstract or may be physically defined by motor properties or consist of nonvisual sensory properties. The nonvisual category will pertain to physically defined nonvisual properties (tactile, olfactory, auditory and gustatory properties) (Farah and McClelland, 1991) and more abstract domains.

Besides the category of the probe noun and the type of property, a key characteristic of a property verification question is the association strength between the noun and the property. The associative strength determines the ease and rapidity with which a judgment can be made and the semantic control demands. In the current experiment we examined to which degree the perirhinal semantic similarity effect depended on the association strength between noun and property, as a proxy for the degree of semantic control demands.

Semantic similarity of a word set can be modelled in various ways. In previous studies (Bruffaerts et al., 2013; Liuzzi et al., 2015, 2017; Martin et al., 2018) a concept-feature matrix was derived from responses of a large group of individuals obtained during a feature generation task (De Deyne et al., 2008). In another study semantic similarity was derived from word co-occurrences in text corpora (Martin et al., 2018). To further evaluate the generalisability of the perirhinal findings we modelled the semantic similarity in the current experiment based on a random walk through a graph of words constructed starting from responses to a word associate task performed online by more than 70,000 participants (De Deyne et al., 2013, 2018). De Deyne et al. (2018) compared the latter method with methods based on concept-feature matrices for judging semantic similarity between words (McRae et al., 2005; Devereux et al., 2014). They (De Deyne et al., 2018) found that association measures explained performance on explicit semantic similarity judgments of concrete nouns better than the concept-feature matrix based methods did. Putatively, it may contain information that is less present in concept-feature matrices, such as thematic information (De Deyne et al., 2018).

As a further test of generalisability the perirhinal VOI was defined differently from earlier studies (Bruffaerts et al., 2013; Liuzzi et al., 2015,

2017) based on the Brainnetome atlas (Fan et al., 2016), which integrates information from structural and functional connectivity as well as task-related functional MRI.

## 2. Subjects and methods

### 2.1. Participants

Eighteen subjects (13 women, 5 men) between 18 and 28 years participated in this fMRI experiment. All subjects were native Dutch speakers, right-handed, free of neurological or psychiatric history and had normal hearing and vision. All the procedures were approved by the Ethics Committee of the University Hospital of Leuven.

### 2.2. Experimental design

#### 2.2.1. Task

Subjects performed a property verification task (Fig. 1A and B). Each trial consisted of a sample phase during which one of 24 entities was presented, followed by a 400 ms delay and a property verification question. The study had a  $2 \times 2 \times 2$  factorial design, with three factors: type of property (visual versus nonvisual), input-modality (written word versus picture) and category (animate versus inanimate). In this paper the concrete concepts used in the fMRI study, will be referred to as “entities”.

Each trial started with a blue fixation point (duration 400 ms) followed by the entity, represented as either a written word or a picture (duration 750 ms). Next a yellow fixation point was shown for 400 ms followed by the property verification question which was present on the screen for 900 ms followed by a 2000 ms response window indicated by a purple fixation point. Finally, a white fixation point was present on the screen until the next trial started (4050 ms). The total inter-trial interval was 8500 ms (Fig. 1A and B). The purple fixation point defined the response window: subjects kept a response box in their right hand and were asked to press a lower or upper button to express their “yes” or “no” decision when the fixation point turned to purple. This was counter-balanced between subjects. In order not to miss answers of fast readers, responses were recorded from 300 ms after the onset of the property verification question to 2900 ms. For each property, half of the responses were positive and half were negative.

#### 2.2.2. Entities and properties

The entities and the properties originated from two concept-feature matrices collected by De Deyne and Storms (2008), one for animate, one for inanimate entities. For each category, three subcategories were probed: Mammals, birds, insects for the animate category and kitchen tools, clothes, and music instruments for the inanimate category (Fig. 2). Each subcategory consisted of 4 entities (twenty-four entities in total). For each subcategory four distinctly visual properties (range: mean < 2.5 out of 7) and four distinctly non-visual properties (range: mean > 5.5 out of 7) were selected (forty-eight properties in total) (see Supplementary Material - Section 1 - for a full description of the procedure for property selection). Based on the properties selected, 4 concrete nouns for each subcategory were selected in such a way that half of the correct responses to the property verification task for a given subcategory were positive and half were negative. Word length of the concrete nouns was between 3 and 10 characters. For the entities, log-transformed word frequency of the lemma counts from the Dutch version of the CELEX database (Baayen et al., 1993) was between 0.95 and 3.85, age of noun acquisition between 3.38 and 10.26 years and familiarity between 2.23 and 4.57 (on a 7-point Likert-type scale (De Deyne and Storms, 2008)).

Each property was presented as a fully grammatical sentence (e.g. heeft zes poten (has six paws)). “x” and “+” were added at the beginning and end of each string so that the total string length always was 14 and 29 for the written entity and the property verification question, respectively

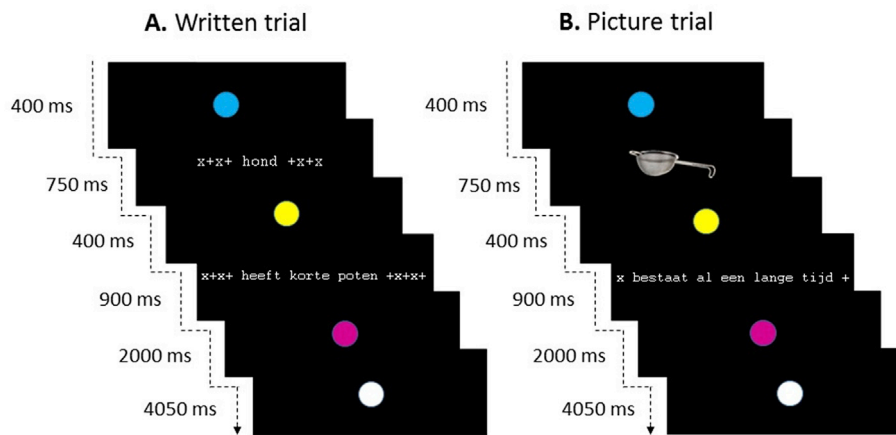


**Fig. 1.** Task. A. Property verification task with entity in written modality. B. Property verification task with entity as picture. English Translation: hond: dog; heeft korte poten: has short legs; bestaat al een lange tijd: exists since long time.

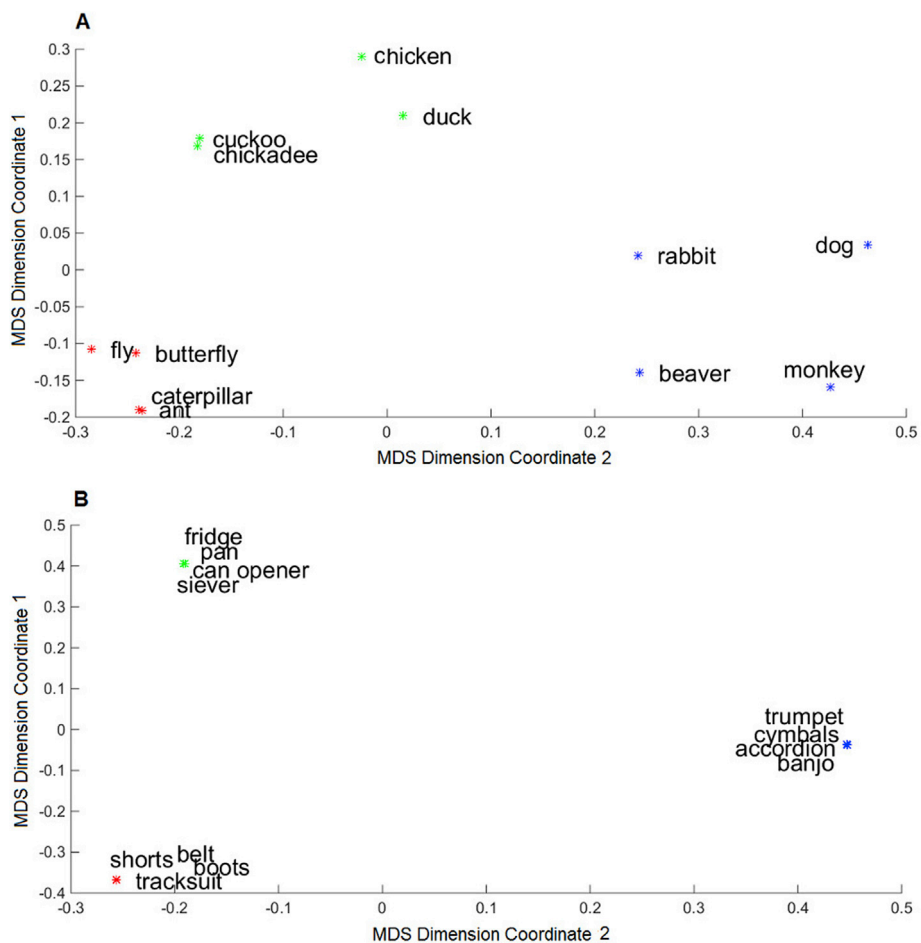


**Fig. 2.** MDS Visual representation of the semantic clusters and semantic distances between entities of animate and inanimate entities, based on the feature generation data collected by De Deyne and Storms (2008). For visualization, data reduction of the similarity matrix to two dimensions was performed by means of multidimensional scaling (MDS).

(Fig. 1A and B). Visual and nonvisual property verification questions did not differ in number of characters ( $P = 0.14$ ) nor in number of words ( $P = 0.66$ ). Written words were presented with a letter size of 0.7 visual degrees. Each picture was presented as prototypical colour photo with size of  $5.1 \times 5.1$  visual degrees. Pictures were selected from a standard picture library (Hemera Photo-Object 5000).

### 2.2.3. Semantic similarity matrix of the entities used

The semantic similarity between the entities was estimated based on a word association database (De Deyne et al., 2013, 2018). This database contains more than 12,000 cue words for which more than 70,000 participants have been asked to provide three different associates per cue (multiple - responses free association task). The association strength was

transformed using positive pointwise mutual information (De Deyne et al., 2016). The latter procedure gives a higher weight to associations that are specific for a given cue than those that occur more generally across different cues (De Deyne et al., 2016). In order to capture the deeper semantic structure, the similarity between each pair of words was estimated by calculating the cosine similarity between the distributions induced when each word was used as seed of a random walk over the network. The distributions included both direct and indirect paths (De Deyne et al., 2016).

For comparison, we calculated the Spearman correlation between the semantic similarity matrix derived from association data and the one derived from concept-feature data (De Deyne et al., 2008): a significant correlation was found for both categories (animate:  $\rho = 0.8$ ,  $P = 0$ ; inanimate:  $\rho = 0.78$ ,  $P = 0.0001$ ).

We formally tested whether there was any relationship between the semantic and the orthographical similarity between the nouns used. The semantic cosine similarity matrix was converted into a dissimilarity matrix by subtracting 1 from each cosine similarity value (1-cosine similarity) and correlated with the orthographic distance matrix obtained by using the Levenshtein distance (Levenshtein, 1966) normalized on the length of the shortest alignment (Heeringa, 2004). No orthographic effect was detected ( $\rho = -0.01$ ,  $P = 0.57$ ).

#### 2.2.4. Association strength between entities and properties

The association between the concept and the property is an important variable characterizing a concept-property pair. The strength of the association of each entity-property pair was estimated by calculating the cosine similarity after random walk between entities and properties based on word association data (De Deyne et al., 2013) (See Supplementary Material - Section 2 - for a full description of how association strength was determined). A paired *t*-test showed a significantly higher association strength for combinations with visual properties (mean = 0.11, SD = 0.04) versus combinations with nonvisual properties (mean = 0.07, SD = 0.04) ( $P = 0.0002$ ).

#### 2.2.5. Number of trials and runs

The fMRI experiment consisted of 8 runs. Each run (255 scans) was composed of 60 trials. These trials (duration 8500 ms each) were: 24 property verification trials with the entity as a written word, 24 with the entity as a picture, and 12 null trials. Null trials consisted of a white fixation point which the subject had to fixate. Across all 8 runs each concept appeared 16 times: 8 times as a written word and 8 times as a picture. Also, each concept was combined with each property once per modality.

Before performing the fMRI experiment, all subjects except the first two performed a practice run outside the MRI scanner, using entities and properties that were not used during the experiment itself.

### 2.3. Behavioral analysis

In order to evaluate how reliably subjects performed the task and to gain insight in the task demands, reaction times and accuracies were analyzed by means of a 3-way Repeated-Measures ANOVA with three within-subjects factors: Input-modality (two levels: written words and pictures), property type (two levels: visual and nonvisual) and category (two-levels: animate and inanimate). The reaction times were calculated from the onset of the probe question. Accuracy of responses was derived by calculating the number of correct answers divided by the total amount of responses. As subjects were instructed to provide an answer to each trial even when they were not completely sure about the correct answer, trials for which an answer was not provided were not taken into account. The Spearman correlation between reaction times and the entity-property association strength was also determined. The first two subjects were excluded from the behavioral analysis because they did not perform the practice session due to technical problems.

### 2.4. Image acquisition

A Philips Achieva dstream 3T equipped with an 32-channel head volume coil provided functional and structural images. Structural imaging sequences consisted of a T1-weighted 3D turbo-field-echo sequence (repetition time = 9.6 ms, echo time = 4.6 ms, in-plane resolution = 0.97 mm, slice thickness = 1.2 mm). Functional images were obtained using T2\* echoplanar images comprising 36 transverse slices (repetition time = 2 s, echo time = 30 ms, voxel size  $2.75 \times 2.75 \times 3.75 \text{ mm}^3$ , slice thickness = 3.75 mm, Sensitivity Encoding (SENSE) factor = 2), with the field of view (FOV) ( $220 \times 220 \times 135 \text{ mm}^3$ ) covering the entire brain. Each run was preceded by 4 dummy scans to reach a steady state magnetization for the BOLD acquisition.

### 2.5. Image preprocessing

The images were analyzed with Statistical Parametric Mapping SPM8 (Wellcome Trust Centre for Neuroimaging, University College London, UK). First, the data were realigned and resliced and a mean functional image was created. Scans were corrected for slice acquisition time. Next, the structural image was co-registered with the mean functional image and segmented in gray matter, white matter and cerebrospinal fluid. Based on the warping parameters obtained during the segmentation step, the functional images were normalized to the Montreal Neurological Institute (MNI) space and resliced to a voxel size of  $3 \times 3 \times 3 \text{ mm}^3$  (Friston et al., 1995). The normalization was also applied to the structural image which was resliced to a voxel size of  $1 \times 1 \times 1 \text{ mm}^3$ . For the univariate analysis, functional images were smoothed using a Gaussian filter with a kernel size of  $5 \times 5 \times 7 \text{ mm}^3$ . We used standard SPM8 modelling to remove covariates of no interest (motion regressors, low-frequency trends).

For the univariate analysis, the fMRI data were modelled using a General Linear Model (GLM) with nine event types. The nine event types corresponded to the different possible combinations of property type (visual or nonvisual), input modality (written words or pictures) and category (animate or inanimate).

For the MVPA procedure, normalized unsmoothed data were modelled using a GLM with the same nine event types as previously described. The entity-property association strength was convolved with the HRF and included in the model as covariate of no interest. Accordingly, the resulting time series was corrected in each voxel for entity-property association strength and movement parameters. We also verified the results without entity-property association strength as regressor.

### 2.6. Perirhinal cortex

Perirhinal cortex was defined based on the Brainnetome Atlas (<http://atlas.brainnetome.org>) (Fan et al., 2016). Parcels 109 and 111 of Brainnetome Atlas corresponding to left rostral area 35/36 and left caudal area 35/36 were extracted and merged. Each VOI was intersected with the individual's gray matter (GM) map. Per individual, only voxels containing more than 50% of gray matter were included in the VOI (Table 1; Fig. 3).

**Table 1**

Number of voxels (voxel size:  $3 \times 3 \times 3 \text{ mm}^3$ ) and standard deviation (S.D.) for each VOI are calculated over 18 participants.

Number of voxels per VOI		
	Average	S.D.
Left Perirhinal cortex	82.7	5.32
Left Parahippocampal gyrus	67.2	4.83
Left Caudal Hippocampus	152.2	11.4
Left Rostral Hippocampus	147.8	4.5
Right Perirhinal cortex	80.9	7.5

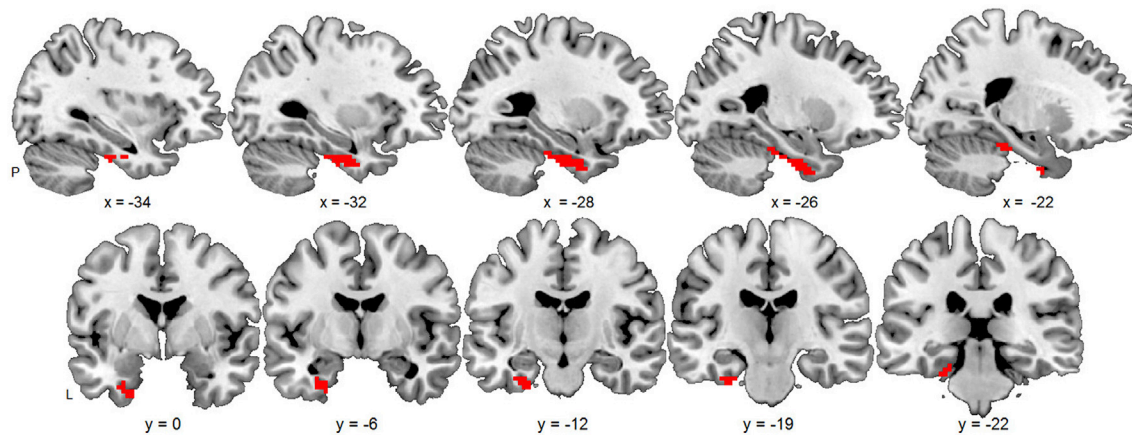


Fig. 3. Left perirhinal cortex superimposed on the GM template of SPM12. Left Perirhinal VOI corresponding to parcel 109 and 111 of Brainnetome Atlas (<http://atlas.brainnetome.org>).

### 2.7. Representational similarity analysis (RSA)

The primary research questions were

1. Is the semantic similarity effect that we previously described in left perirhinal cortex for written words (Bruffaerts et al., 2013; Liuzzi et al., 2015) replicable with a newly defined perirhinal VOI, a new set of nouns, both animate and inanimate, and properties, both visual and nonvisual, and using a different way to model the semantic similarity between entities?
2. Do the semantic similarity effects in the left perirhinal cortex differ when entities are combined with visual versus nonvisual properties for written words and pictures, respectively?
3. Does the semantic similarity effect in perirhinal cortex differ between animate and for inanimate entities?

For each trial, a whole-brain fMRI activation map was created by (a) extracting, for each voxel, the time series corrected for entity-property association strength and for movement parameters, and by (b) calculating the integral of the BOLD signal between 2 and 8 s after the start of the concrete entity within every voxel (fMRI response patterns).

As we were specifically interested in the semantic similarity effect in the left perirhinal VOI, we applied the perirhinal VOI to the activity map of each trial and we calculated the cosine similarity between each pair of trials based on the response pattern in the perirhinal VOI (trial-by-trial matrix). The Spearman correlation was calculated between the lower-triangle part of the semantic cosine similarity matrix (see above) and the lower-triangle part of each fMRI similarity matrix. The diagonal of the matrices, which consisted of pairs of the same entities, were excluded from the computation. The fMRI similarity matrix was created by selecting from the trial-by-trial matrix the cosine similarity values of a specific pair of entities and averaging them within subjects and across subjects.

In order to address question 1, we examined the correlation between the semantic similarity matrix and the fMRI cosine similarity matrix for written words in the left perirhinal VOI. We also examined whether it was present in each of the two constituent parts: the rostral and the caudal part. We also examined the correlation between the semantic similarity matrix and the fMRI cosine similarity matrix for pictures, for visual and nonvisual properties separately and for animate and inanimate entities separately. In case a significant semantic similarity effect was detected, we examined the correlation between the semantic similarity matrix and fMRI cosine similarity matrices for the different constituent combinations of input-modality, property type and category.

In order to address our a priori questions 2 and 3, we examined whether the semantic similarity effect in left perirhinal cortex differed

significantly between visual and nonvisual property verification for written words and pictures, respectively. In addition, we examined whether the semantic similarity effect differed between animate and inanimate entities. The significance of the difference between semantic similarity effects was tested by calculating, for each effect, the RSA at individual level and computing the significance of the difference of individual's correlation values by using a non-parametric test (Wilcoxon signed-rank test). The significance of the Spearman correlation between the fMRI similarity matrix and the semantic cosine similarity matrix was determined by comparing the true correlation with 10,000 possible correlation values obtained by random labelling (random permutation labelling). We used a one-tailed statistical threshold of  $P < 0.05$  uncorrected.

All effects were determined after correction for movement parameters and association strength. We also verified the effects observed by performing an analysis with correction for movement parameters only. The RSA was then re-computed.

When significant effects were found, we verified the results by performing the correlations between the semantic similarity matrix and the fMRI similarity matrix at subject level and evaluating the significance across subjects. A subject-specific fMRI similarity matrix was created by selecting from the trial-by-trial matrix the cosine similarity values of a specific pair of entities and averaging them within subject. The Spearman correlation was calculated between the lower-triangle part of the semantic cosine similarity matrix (see above) and the lower-triangle part of each subject-specific fMRI similarity matrix. The diagonal of the matrices, which consisted of pairs of the same entities, were excluded from the computation. Inferential statistical analyses were performed using a one-sided Wilcoxon signed-rank test across subject-specific RSA correlations.

### 2.8. Left parahippocampal gyrus, caudal and rostral hippocampus and right perirhinal cortex

In order to determine the anatomical specificity of the semantic similarity effect for written words, the effect of semantic similarity was also determined in the left parahippocampal gyrus, left rostral hippocampus, left caudal hippocampus and right perirhinal cortex. All regions were extracted from the Brainnetome Atlas (<http://atlas.brainnetome.org>) (Fan et al., 2016): The left parahippocampal gyrus corresponds to parcels 113 and 119, the left caudal hippocampus corresponds to parcel 217, the left rostral hippocampus to parcel 215 and the right perirhinal cortex to parcel 110 and 112 of Brainnetome Atlas (Fig. 4). Each VOI was intersected with each individual's GM map. Per subject only voxels containing more than 50% of gray matter were included in the VOI (Table 1).

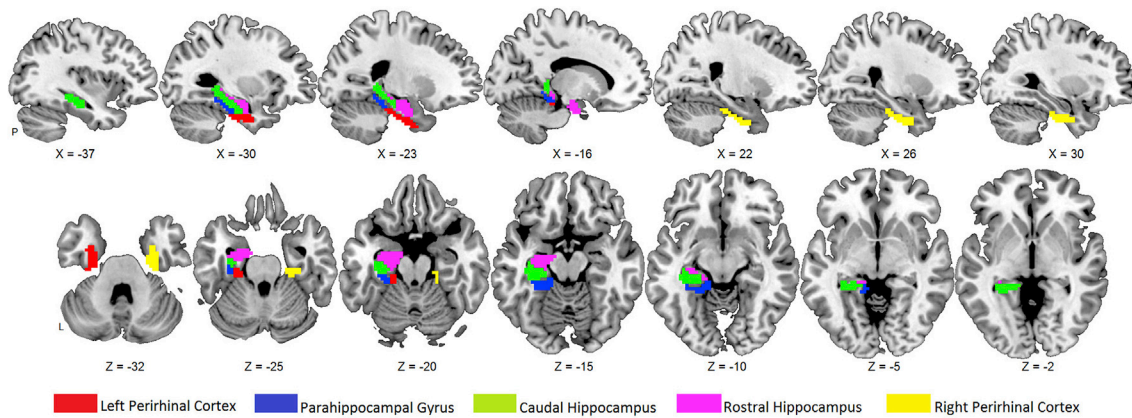


**Fig. 4.** Neighbour regions of the left perirhinal cortex and right perirhinal cortex intersected with GM template of SPM12. Binary representation of the left perirhinal cortex (*red*). Left parahippocampal gyrus (*blue*). Left Caudal hippocampus (*green*). Left Rostral hippocampus (*purple*). Right Perirhinal Cortex (*yellow*).

2.9. Whole-brain analysis

In order to evaluate the brain activity context against which the perirhinal effects occurred during visual and nonvisual property retrieval, we will also report the main effect of property type (Visual *minus* NonVisual and inverse contrast). This was based on a whole-brain univariate analysis. The main effect of category and of input-modality are reported in the Supplementary Material (Supplementary Material - Section 3). Second, we will also report the effect of the entity-property

association strength. Entity-property association strength values were convolved and included as regressor in a separate GLM with 4 event types each: (1) Property verification trials for written words, (2) property verification trials for pictures, (3) null trials, (4) convolved entity-property association strength. We will also report the parametric analysis with association strength.

For all whole-brain analyses, the significance level was set at a voxel-level inference threshold of uncorrected  $P < 0.001$  combined with a cluster-level inference of  $P < 0.05$  corrected for the whole brain volume

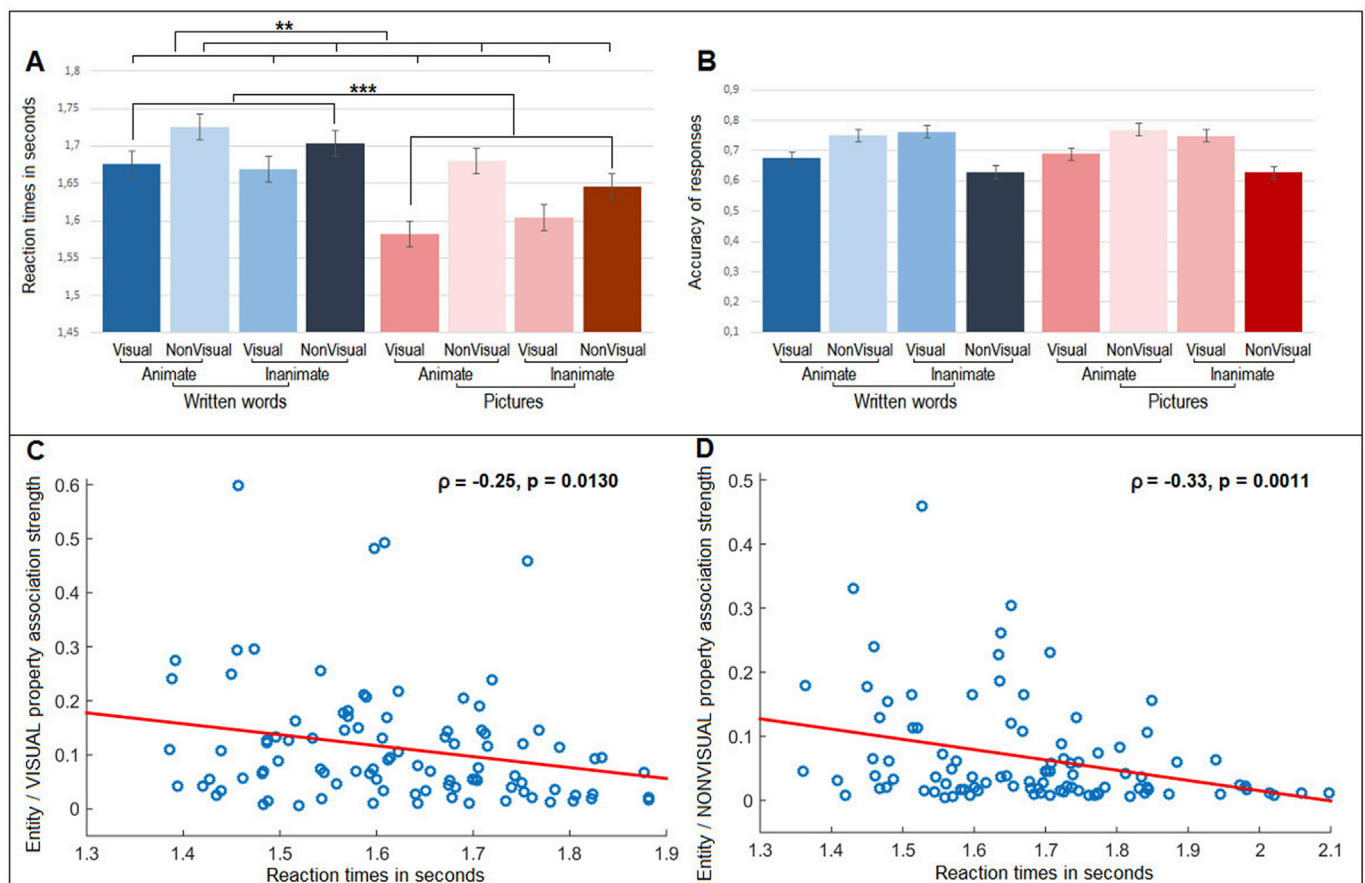


**Fig. 5.** Behavioral data. A. Reaction times calculated from the probe question onwards. X axis: eight experimental conditions. Y axis: reaction times in seconds. \*\* corresponds to  $P < .001$ . \*\*\* corresponds to  $P < .0001$ . Error bars indicate the standard error. B. Accuracy of responses - X axis: eight experimental conditions. Y axis: correct answers divided by the total amount of responses provided. Error bars indicate the standard error. C. Spearman correlation between the entity/visual property association strength and the reaction times. D. Spearman correlation between the entity/nonvisual property association strength and the reaction times.

(Poline et al., 1997). To examine effects occurring within the perirhinal VOI, the significance level was set at corrected  $P < 0.05$  using small volume correction (SVC).

### 3. Results

#### 3.1. Behavioral analysis

A 3-way repeated measures ANOVA with three factors - input-modality (two levels: written words and pictures), property type (two levels: visual and nonvisual), and category (two levels: animate and inanimate) - showed a main effect of input-modality on reaction times: Subjects were significantly faster when the entity was presented as a picture (1.63 s,  $SD = 0.04$ ) than as a written word (1.69 s,  $SD = 0.03$ ) ( $F(1,15) = 31.9$ ;  $P = 0.000$ ). The main effect of property type was significant: Subjects were significantly faster when the property to be verified was visual (1.63 s,  $SD = 0.05$ ) compared to nonvisual (1.68 s,  $SD = 0.03$ ) ( $F(1,15) = 17.60$ ;  $P = 0.001$ ). No main effect of category was present ( $F(1,15) = 0.7$ ;  $P = 0.39$ ). The interaction between property type and input-modality (written words versus pictures) was significant ( $F(1,15) = 5.3$ ;  $P = 0.035$ ). The Tukey posthoc analysis did not show any significant effects. There were no significant other interactions ( $P > 0.06$ ) (Fig. 5A).

A 3-way repeated measures ANOVA with accuracy as outcome measure showed a main effect of category: Subjects were more accurate when the entity was an animate entity (accuracy = 0.71,  $SD = 0.08$ ) compared to an inanimate entity (accuracy = 0.68,  $SD = 0.09$ ) ( $F(1,15) = 4.63$ ;  $P = 0.048$ ). There was no main effect of input-modality or property type ( $P > 0.10$ ). The interaction between category and property type was significant ( $F(1,15) = 47.24$ ;  $P = 0.0005$ ) (Fig. 5B).

A linear regression analysis revealed a significant negative correlation between reaction times and the association strength between entity and property ( $\rho = -0.33$ ,  $P = 0.000004$ ). This effect was present both for visual property trials ( $\rho = -0.25$ ,  $P = 0.0130$ ) (Fig. 5C) and for nonvisual property trials ( $\rho = -0.33$ ,  $P = 0.0011$ ) (Fig. 5D).

#### 3.2. Perirhinal cortex

In left perirhinal cortex (Fan et al., 2016) the semantic similarity effect for the written words trials was significant ( $\rho = 0.16$ ,  $P = 0.0054$ ) (Table 2, Fig. 6A). A significant semantic similarity effect for written words was detected in both the caudal and the rostral part of the left perirhinal cortex (caudal:  $\rho = 0.18$ ,  $P = 0.0039$ ; rostral:  $\rho = 0.24$ ,  $P = 0.042$ ). When association strength was not included as a covariate of no interest in the RSA, the results remained essentially the same ( $\rho = 0.14$ ,  $P = 0.015$ ). When the correlation between the semantic similarity matrix and the fMRI similarity matrix was determined at the single subject level, the effect size was much lower, the semantic similarity

**Table 2**

RSA in left perirhinal VOI. RSA values which reached significance set at  $P < 0.05$  are marked in bold.

RSA: Left perirhinal VOI		
	$\rho$	P-value
Written words	<b>0.16</b>	<b>0.0054</b>
Pictures	0.04	0.26
Visual	0.08	0.1
NonVisual	0.02	0.36
Animate	0.07	0.29
Inanimate	0.18	0.06
Written words/Visual properties	0.09	0.06
Written words/NonVisual properties	-0.02	0.58
Pictures/Visual properties	0.02	0.36
Pictures/NonVisual properties	-0.0004	0.5
Written words/Animate	-0.17	0.9
Written words/Inanimate	<b>0.39</b>	<b>0.0015</b>

effect for written words however remained significant (mean  $\rho = 0.03$ ,  $P = 0.02$ ) (Table 3, Fig. 7).

When written words referring to inanimate entities were tested separately, a significant semantic similarity effect was detected ( $\rho = 0.39$ ,  $P = 0.0015$ ). This was not the case for written words referring to animate entities ( $\rho = -0.17$ ,  $P = 0.91$ ). The difference in semantic similarity effect between written words referring to animate entities and written words referring to inanimate entities was significant ( $P = 0.0074$ ).

No significant semantic similarity effects were detected for pictures ( $\rho = 0.04$ ,  $P = 0.26$ ) (Table 2, Fig. 6B). The difference in semantic similarity effect between written word trials and picture trials was not significant ( $P > 0.4$ ), nor was there a significant difference between visual and nonvisual property verification ( $P > 0.5$ ), nor between animate and inanimate entities ( $P > 0.3$ ) (Fig. 6).

None of the univariate contrasts revealed significant effects in perirhinal VOI.

#### 3.3. Semantic similarity effects in left parahippocampal gyrus, caudal and rostral hippocampus and right perirhinal cortex

In the left parahippocampal gyrus the semantic similarity effect for written words was significant ( $\rho = 0.17$ ,  $P = 0.0047$ ). This was not the case for the left caudal hippocampus ( $P > 0.1$ ), the left rostral hippocampus ( $P > 0.1$ ) and the right perirhinal cortex ( $P > 0.07$ ).

When the semantic similarity effect for written words in left perirhinal cortex was compared directly to the semantic similarity effect for written words in left parahippocampal gyrus, the hippocampal regions or the right perirhinal cortex, no significant differences were found between the regions.

#### 3.4. Whole-brain analysis

Visual compared to nonvisual property verification (contrast: Visual *minus* NonVisual) activated the lateral occipital cortex and the middle segment of the intraparietal sulcus bilaterally as well as the fusiform gyrus to the left, in line with the a priori hypothesis (Table 4, Fig. 8A). Inversely, nonvisual compared to visual property verification (contrast: NonVisual *minus* Visual) activated an extensive left-hemispheric zone which extended from left angular gyrus over the superior temporal sulcus from its posterior to its anterior end to the anterior inferior frontal gyrus, the superior frontal gyrus and also included the posterior cingulate. To the right, the superior temporal sulcus up to its anterior end and the anterior IFG were also more active for nonvisual compared to visual properties (Table 4; Fig. 8B). When association strength or reaction times were included as parametric modulators, the contrasts between visual and nonvisual property verification yielded essentially the same results as when no parametric modulators were included (Table 4).

Association strength between entity and property correlated positively with fMRI activity bilaterally in the inferior temporal cortex and the intraparietal sulcus and in the left supramarginal gyrus (Fig. 9A). Inversely, lower association strength correlated with higher activity levels in the left IFG, superior frontal gyrus and the orbital part of the right IFG (Table 5, Fig. 9B).

The univariate analyses with small-volume correction for the perirhinal cortex did not yield any significant effects.

### 4. Discussion

Overall the presence of a perirhinal semantic similarity effect was more determined by the input-modality than by the content of the retrieved knowledge or the semantic control demands. The semantic similarity effect for written words in left perirhinal cortex is a robust and replicable finding. Contrary to our a priori hypothesis, the type of property retrieved, visual versus nonvisual, did not alter the semantic similarity effect in left perirhinal cortex for pictures or for words. The degree of cognitive control required, as determined by the entity-

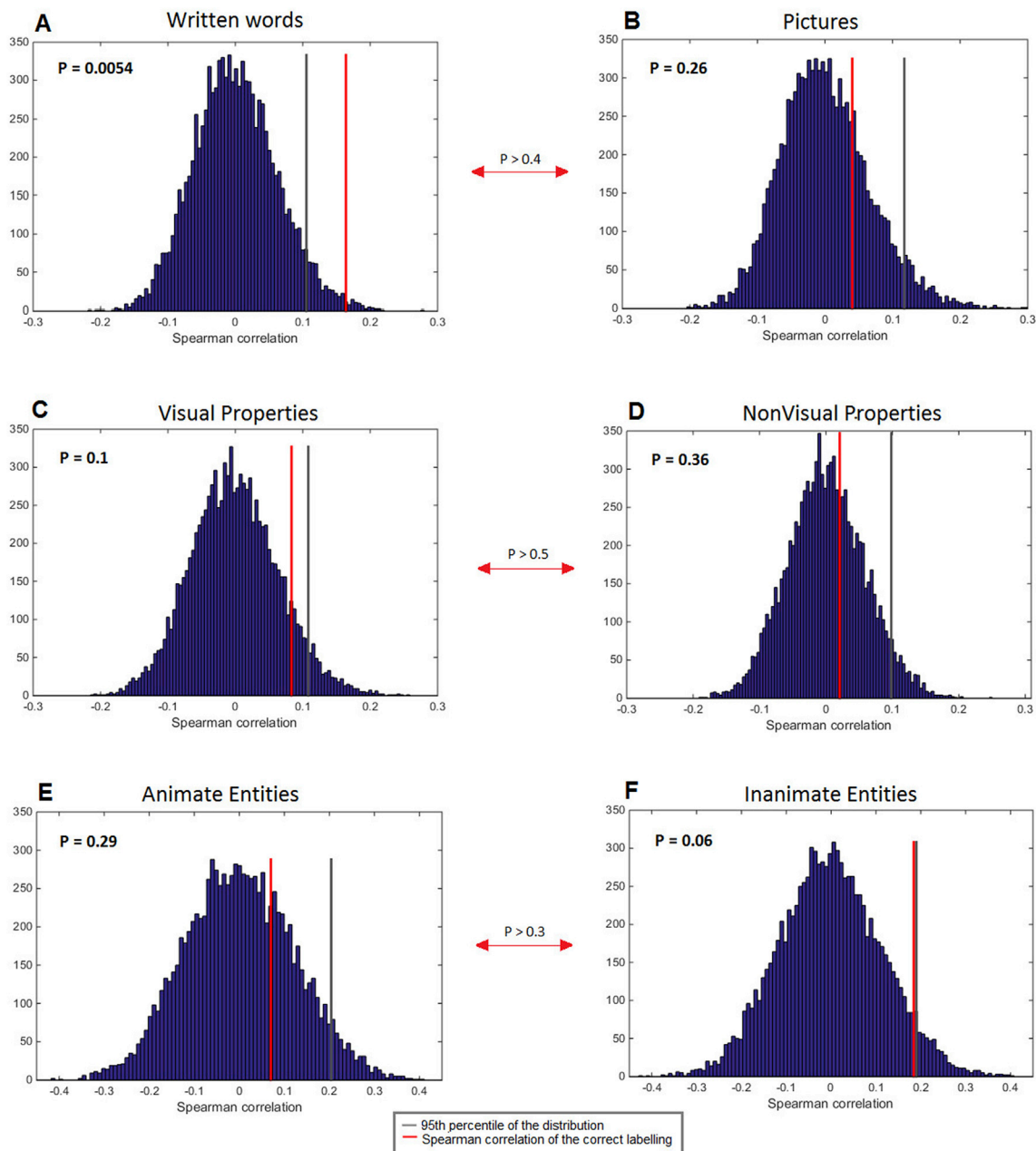


**Fig. 6.** Semantic similarity effects in left perirhinal cortex. Probability distributions for the representational similarity analysis (RSA) between the semantic cosine similarity matrix and the fMRI cosine similarity matrix for (A) written words after random labelling, (B) pictures after random labelling, (C) visual properties after random labelling, (D) nonvisual properties after random labelling, (E) animate entities after random labelling and (F) inanimate entities after random labelling. The red line indicates the Spearman correlation coefficient between the similarity matrix based on behavioral data and the similarity matrix based on the fMRI data derived from the response patterns within the left perirhinal VOI. The gray line indicates the 95th percentile of the distribution. X-axis: correlation averaged over the group of subjects. Y-axis: absolute frequency of a given Spearman correlation value across a total of 10,000 random permutation labellings.

property association strength, also did not have an effect on the semantic similarity effect in perirhinal cortex. Univariate analysis revealed a strong double dissociation between explicit retrieval of visual versus nonvisual properties and a strong effect of association strength in prefrontal regions but not in perirhinal cortex.

The current study replicates earlier findings (Bruffaerts et al., 2013; Liuzzi et al., 2015, 2017; Martin et al., 2018) for a novel set of nouns and properties across a wider range of properties and categories and a wider range of noun-property association strengths. The anteromedial ventral temporal VOI in Bruffaerts et al. (2013) contained the posterior half of perirhinal cortex, part of the parahippocampal gyrus and extended medially in the hippocampus (Liuzzi et al., 2015). In a follow-up study

(Liuzzi et al., 2015), the result was verified in a manually delineated VOI restricted to left perirhinal cortex based on the Kivisaari et al. (2013) procedure (Kivisaari et al., 2013). Here, the perirhinal VOI was anatomically defined based on the Brainnetome Atlas (Fan et al., 2016). As a further difference, the semantic similarity was based on a graph-based model of word associations derived from a cued word associate task and a random walk (De Deyne et al., 2013, 2016) rather than a feature-concept matrix derived from feature generation (De Deyne et al., 2008). Despite all these differences, the results of the current study replicated the effect of semantic similarity for concrete written words in left perirhinal cortex (Bruffaerts et al., 2013; Liuzzi et al., 2015). Recently, a study from a different centre came to the same conclusions

**Table 3**

Subject-level RSA in the left perirhinal VOI. The mean value is obtained by averaging individual Spearman correlations values between the behavioral matrix and the fMRI similarity matrices. Significance set at  $P < 0.05$  are marked in bold.

Subject-level RSA: Left perirhinal VOI		
	Mean $\rho$	P-value
Written words	<b>0.03</b>	<b>0.02</b>
Pictures	0.01	0.4
Visual	0.02	0.3
NonVisual	0.003	0.6
Animate	0.008	0.5
Inanimate	0.04	0.08

(Martin et al., 2018). In that study, a semantic similarity effect was found for written words in perirhinal cortex, regardless of how the similarity between written words was modelled: Based on subjective estimates of the visual similarity between the words' referents or based on a conceptual similarity based on a corpus of words (Martin et al., 2018). In contrast to Martin et al. (2018), we found a semantic similarity effect also in the neighbouring parahippocampal gyrus to the left. This suggests that semantic similarity effects gradually emerge from the anterior ventromedial occipitotemporal processing stream, rather than being confined to one discrete area. The left parahippocampal gyrus is one of the major connections of the perirhinal cortex and intrinsically subserves contextual information (Bar et al., 2009).

A semantic similarity effect was also present for written words referring to inanimate compared to animate entities, opposite to our a priori hypothesis. It is important to point out that the total number of trials for each of these conditions is only 96 (out of 384) per subject. Given the unexpected direction of the effect and the relatively low number of trials on which this sub-analysis is based, the effect of category on the written word semantic similarity effect would require replication in a confirmatory experiment. By considering the nature of the properties and the semantic categories (animals and manipulable objects) adopted in this study, we could speculate that a semantic similarity effect for written words referring to inanimate entities can be ascribed to an integrative process related to the retrieval of attributes that are less closely associated with a concept: When manipulable objects - which mostly rely on functional attributes - are probed with sensory visual,

sensory nonvisual and abstract attributes, an integrative process is triggered (Martin et al., 2018). An identical phenomenon should be expected for written words referring to animals, but since for half of the trials animals were probed with visual properties and visual properties may have a relatively higher weight in the semantic representation of animals compared to manipulable objects, the demands for integrative processing could possibly have been lower. As mentioned above, confirmatory experiments are needed.

According to the a priori hypothesis that generated the current experiment, the type of property retrieved, visual or nonvisual, could have determined whether a semantic similarity effect were found for pictures too. When nonvisual properties are retrieved, the structural description system may not suffice to solve the task and more anterior temporal processing might be required for pictures too. This hypothesis could not be confirmed. Our data should by no means be thought to imply that perirhinal cortex does not play a role in semantic processing of nonverbal objects. Perirhinal cortex has a well-established role in processing of visual objects, especially when similarity between objects is high (Bright et al., 2004; Liu et al., 2009; Peelen and Caramazza, 2012; Tyler et al., 2013). Hence our current claim is not at all that perirhinal cortex is only involved in the processing of written words. There is ample evidence for the role of perirhinal cortex in object processing, both from functional imaging (Tyler et al., 2004, 2013; Kivisaari et al., 2012; Clarke and Tyler, 2014; Price et al., 2017) and from direct electrophysiological recordings (Quiroga et al., 2005). In the current study, the effect for pictures did not reach significance. This may be related to a number of factors. Repeated exposure to an identical picture during the course of the current experiment without variation in scale or viewpoint (Liu et al., 2009) may have attenuated the effect of semantic similarity on perirhinal responses for pictures. The pictures were also easy to discriminate. Contemporary theories on object processing in perirhinal cortex emphasize its role in disambiguating objects that are confusable and, hence, would even not predict an effect for pictures in our experiment (Clarke and Tyler, 2015).

The study design also allowed us to evaluate the effect of the type of property retrieved as well as the effect of the association strength between the entity and the property queried on the neocortical activity patterns (Martin, 2007; Fernandino et al., 2016). Explicit retrieval of visual properties activated the intraparietal sulcus and ventral and lateral occipital cortex, in line with the embodied cognition model (Martin,

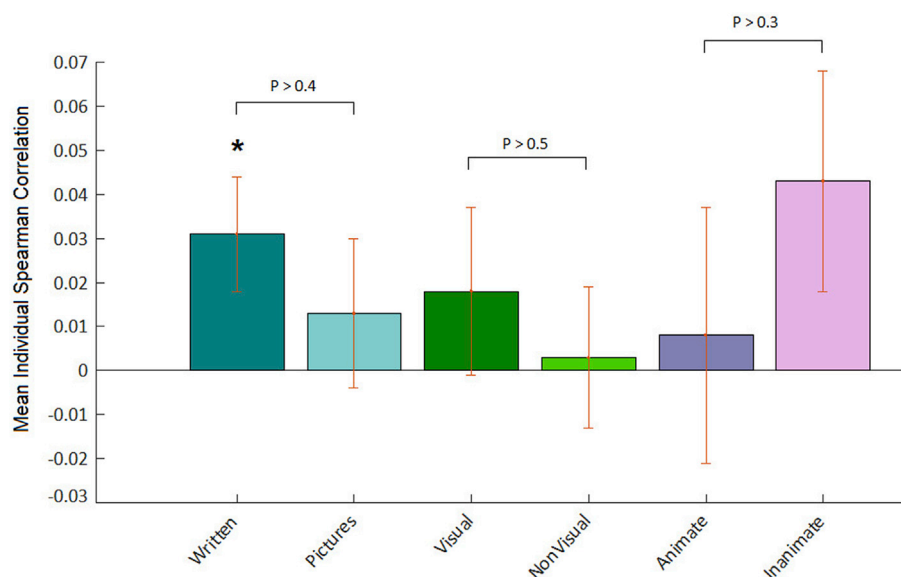


**Fig. 7.** Subject-level RSA: Semantic similarity effects in left perirhinal cortex. The similarity was quantified by means of Spearman correlation between the behavioral matrix and the fMRI similarity matrices. Error bars indicate the standard error of the mean (SEM).  $*p < 0.05$ . The  $p$ -values reported in between of two effects refer to the significance of the difference of the effects indicated.

**Table 4**

Clusters showing a main effect of property type (NonVisual property > Visual property and Visual property > NonVisual property) at a voxel-level inference threshold of uncorrected  $P < 0.001$  combined with a cluster-level inference of  $P < 0.05$  corrected for the whole brain volume (Poline et al., 1997). For clusters composed of more than 1000 voxels, up to three local maxima are shown. Extent refers to the number of  $3 \times 3 \times 3 \text{ mm}^3$  voxels. *Abbreviations:* L: left; R: right; STG: Superior Temporal Gyrus; ATL: Anterior Temporal Lobe; IFG: Inferior Frontal Gyrus.

Main effect of property type					
	MNI			Extent	$P_{\text{FWE-corr.}}$ (cluster-level)
	coordinates				
	x	y	z		
NonVisual <i>minus</i> Visual					
L STG up to ATL and anterior IFG	-45	32	-2	1257	0.000
	-51	23	1		
	-45	14	-32		
L superior frontal gyrus	-18	53	34	516	0.000
R ATL and anterior IFG	48	17	-23	317	0.000
R Superior Temporal Sulcus	48	-22	-5	80	0.003
Posterior Cingulate	-3	-52	22	208	0.000
Visual <i>minus</i> NonVisual					
L Lateral Occipital Cortex	-51	-58	-14	172	0.000
R Lateral Occipital Cortex	51	-52	-14	119	0.000
R Intraparietal Sulcus	33	-67	43	205	0.000
L Intraparietal Sulcus	-30	-61	43	247	0.000
L Fusiform Gyrus	-30	-49	-20	71	0.005

2007; Vandenberg et al., 2006; Fernandino et al., 2015a,b). Retrieval of nonvisual properties activated a distributed network consisting of precuneus, inferior parietal lobule, left superior temporal sulcus and inferior frontal gyrus. When Anderson et al. (2015) analyzed the fMRI pattern for concrete nouns using an image-based versus a text-based model, the regions found for the text-based model were relatively similar to those observed for the contrast of nonvisual minus visual properties in the current study. This leads us to the hypothesis that the pattern during nonvisual versus visual property verification may relate to the higher demands on verbal knowledge and reasoning when retrieving nonvisual properties.

Nonvisual properties activated the anterior inferior frontal gyrus: BA 47 and a small posterior portion of BA 45. Response amplitude in the anterior inferior frontal gyrus correlated negatively with the association

strength between the noun and the property verification question was correlated with the entity properties association strength. An effect for lower association strength in BA 47 is in line with the involvement of this region in semantic control processing (Noonan et al., 2013; Lambon-Ralph et al., 2016). The lower the association strength, the wider the range of possible connections between the noun and the property and the higher the demands placed on the semantic control system (Noonan et al., 2013; Lambon-Ralph et al., 2016). According to the two-process model of lateral prefrontal cortex (Badre and D'Esposito, 2009), BA 47 is activated for high-level control: Whereas BA 44 and 45 are critical regions for selection between competing alternative and inhibiting irrelevant task responses (Badre et al., 2005), BA 47 is critical for determining relevant knowledge for judging a specific semantic association.

#### 4.1. Implications for a written word processing model

We propose a model where the left perirhinal cortex serves as connector hub between the written word input and the distributed representation of its meaning. This hypothesis is in line with the Posterior Medial temporal-Anterior Temporal functional anatomical model (Ranganath and Ritchey, 2012; Ritchey et al., 2015). According to the hypothesis we propose (Liuzzi et al., 2015), the associative coding between a concrete written word and its referent is mediated by the perirhinal cortex based on similar operational principles as the associative coding between paired items as documented in nonhuman primates (Sakai and Miyashita, 1991; Naya et al., 2001, 2003; Hirabayashi et al., 2013; Liuzzi et al., 2015). Next, the paired word-entity activity pattern needs to connect with the distributed neocortical representation of the meaning of the entity. According to this view, the synchronized activity between the written word input and its referent in perirhinal cortex constitutes the link between the written word and the distributed representation of meaning. As the current study shows, this does not depend on the property retrieved, visual versus nonvisual. In contrast, the distributed representation in neocortex is organized according to themes and content. The hypothesis is also of clinical relevance. One of the defining criteria for the semantic variant of primary progressive aphasia (PPA SV) is surface alexia, a clinical syndrome that is characterized by a disconnection between the word form and its meaning (Gorno-Tempini et al., 2011). Of course other routes exist through which written words may access the distributed representations of word meaning, e.g. through

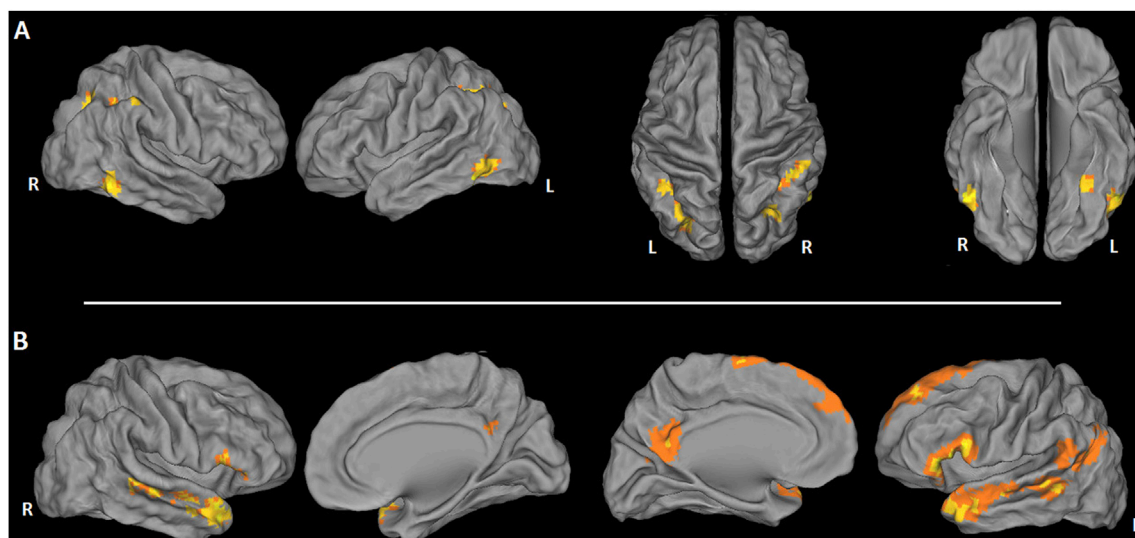


**Fig. 8.** Main effect of property type. A. Visual > NonVisual: 3D rendering of the overall activity map. B. NonVisual > Visual: 3D rendering of the overall activity map. Significant level: voxel-level inference threshold of uncorrected  $P < 0.001$  combined with a cluster-level inference of  $P < 0.05$  corrected for the whole brain volume (Poline et al., 1997).

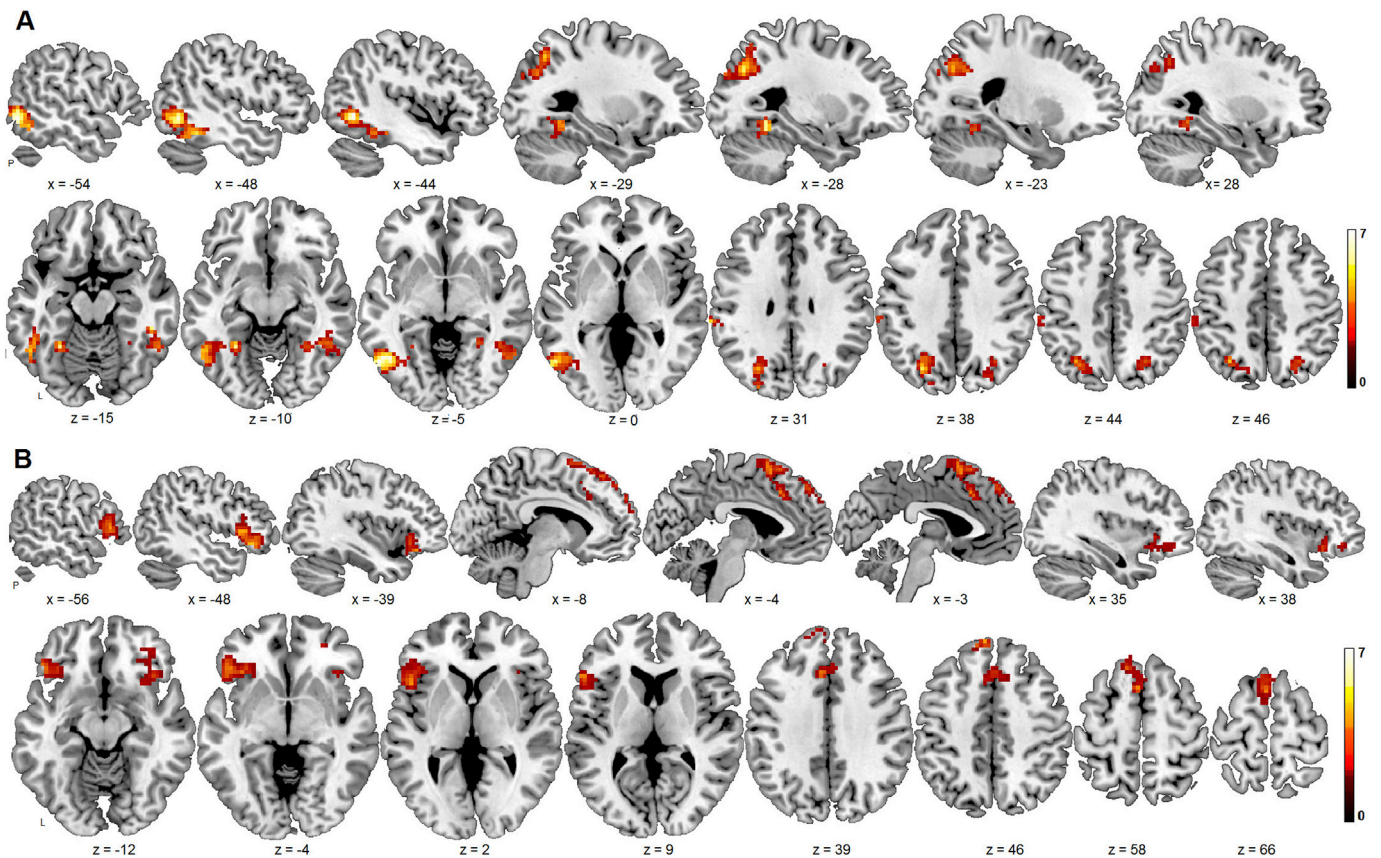


**Fig. 9.** Parametric effect of entity - property association strength. A. Positive correlation between fMRI activity levels and association strength: sagittal and axial slices. B. Negative correlation between fMRI activity levels and association strength: sagittal and axial slices. Significant level: voxel-level inference threshold of uncorrected  $P < 0.001$  combined with a cluster-level inference of  $P < 0.05$  corrected for the whole brain volume (Poline et al., 1997).

**Table 5**

Parametric Analysis: Entity-Property Association Strength - Positive and Negative correlation. Significant level: voxel-level inference threshold of uncorrected  $P < 0.001$  combined with a cluster-level inference of  $P < 0.05$  corrected for the whole brain volume (Poline et al., 1997). For clusters composed of more than 1000 voxels, 3 local maxima are shown. Extent refers to the number of  $3 \times 3 \times 3 \text{ mm}^3$  voxels. Abbreviations: IFG: Inferior frontal gyrus.

Parametric effects of entity - property association strength	MNI			Extent	$P_{\text{FWE-corr.}}$ (cluster-level)
	coordinates				
	x	y	z		
<b>Positive Correlation</b>					
L inferior temporal cortex	-45	-61	-2	278	0.000
R Inferior Temporal cortex	48	-37	-14	118	0.000
L intraparietal sulcus	-27	-70	34	151	0.000
R intraparietal sulcus	27	-64	43	72	0.003
L supramarginal gyrus	-66	-31	28	60	0.004
<b>Negative Correlation</b>					
L IFG	-48	29	-8	307	0.000
L Superior Frontal Gyrus	-6	50	46	331	0.000
R IFG, Orbital part	39	23	-11	75	0.003

grapheme-to-phoneme conversion (Jobard et al., 2003; Shaywitz and Shaywitz, 2008; Wandell et al., 2010). Our model proposes an alternative route that goes as far as perirhinal cortex. According to our model the role of this ventral occipitotemporal stream builds upon the pre-existing functions of the visual object processing pathway. In PPA SV, the anterior temporal pole is atrophic. The atrophy extends across its medial, ventral and lateral surface. Volume loss in PPA SV also includes perirhinal cortex (Mion et al., 2010). In PPA SV cerebral metabolism in the

left anterior fusiform region (including left perirhinal cortex) correlates with behavioral scores on picture naming and category fluency (Mion et al., 2010). It is important to note that in PPA SV the semantic deficit is amodal, i.e. for written and spoken words and, as the disease progresses, also for nonverbal materials. In contrast, the semantic similarity effect we report here in perirhinal cortex is restricted to written words. This can be explained in different ways. As mentioned above, the perirhinal effect may be task-dependent and semantic effects have been found in perirhinal cortex for other modalities too in tasks such as categorization and naming (Kivisaari et al., 2012; Fairhall and Caramazza, 2013; Clarke and Tyler, 2014). Furthermore, the anterior temporal atrophy in SV is much more extensive than perirhinal cortex alone.

**4.2. Study limitations**

Although the effect of semantic similarity was present for written words in the perirhinal cortex and in the parahippocampal gyrus, the direct comparison of the effect between the regions did not reach significance. The absence of these effects probably reflects limitations in sensitivity of the current method.

The association strength between the noun and the property was higher for visual than for nonvisual properties and this correlated inversely with reaction times. Nevertheless, the activity pattern was present even when association strength was included as a covariate.

There may be technical reasons why the semantic similarity effect is significant for written words but not for pictures. For instance, the activity pattern may be more heterogeneous for pictures than for written words due to the heterogeneity in form characteristics in pictures. This variance may obscure similarity effects related to semantic similarity.

In the current study, main results are based on a group-level RSA.

Even so, significant effects were verified by computing the correlation between the semantic similarity matrix and the fMRI similarity matrix at the individual level and determining the significance across subjects. In this way the between-subjects variance is taken into account.

## 5. Conclusion

The left perirhinal effect of semantic similarity for written words is robust and has now been replicated across different sets of nouns and properties, with various definitions of the perirhinal volume and different ways to model semantic similarity as well as different analysis methods. In the current study, the type of property retrieved as well as the association strength between the entity and the property queried had a profound effect on the neocortical involvement but not on the semantic similarity effect in perirhinal cortex. We propose a model where the left perirhinal cortex is a connector hub, connecting the written word input with the distributed representation of word meaning through associative coding between the written word and its referent in left perirhinal cortex.

## Acknowledgements

R.V. is a Senior Clinical Investigator of the Research Foundation Flanders. R.B. is a postdoctoral fellow of the Research Foundation Flanders (FWO). Funded by Federaal Wetenschapsbeleid (Belspo 7/11), FWO (Grant no. G0925.15) and KU Leuven (OT/12/097 and C14/17/108).

## Appendix A. Supplementary data

Supplementary data to this article can be found online at <https://doi.org/10.1016/j.neuroimage.2019.02.011>.

## References

- Anderson, A.J., Bruni, E., Lopopolo, A., Poesio, M., Baroni, M., 2015. Reading visually embodied meaning from the brain: visually grounded computational models decode visual-object mental imagery induced by written text. *Neuroimage* 120, 309–322.
- Baayen, H., Piepenbrock, R., Rijn, H., 1993. The CELEX Lexical Data Base on [CD-ROM]. University of Pennsylvania, Linguistic Data Consortium, Philadelphia.
- Badre, D., D'Esposito, M., 2009. Is the rostro-caudal axis of the frontal lobe hierarchical? *Nat. Rev. Neurosci.* 10, 659–669.
- Badre, D., Poldrack, R.A., Paré-Blagoev, E.J., Insler, R.Z., Wagner, A.D., 2005. Dissociable controlled retrieval and generalized selection mechanisms in ventrolateral prefrontal cortex. *Neuron* 47, 907–918.
- Bar, M., Aminoff, E., Schacter, D.L., 2009. NIH public access. *Psychology* 28, 8539–8544.
- Binder, J.R., Conant, L.L., Humphries, C.J., Fernandez, L., Simons, S.B., Aguilar, M., Desai, R.H., 2016. Toward a brain-based componential semantic representation. *Cogn. Neuropsychol.* 1–45.
- Bright, P., Moss, H., Tyler, L.K., 2004. Unitary vs multiple semantics: PET studies of word and picture processing. *Brain Lang.* 89, 417–432.
- Bruffaerts, R., Dupont, P., Peeters, R., De Deyne, S., Storms, G., Vandenberghe, R., 2013. Similarity of fMRI activity patterns in left perirhinal cortex reflects semantic similarity between words. *J. Neurosci.* 33, 18597–18607.
- Chao, L.L., Haxby, J.V., Martin, A., 1999. Attribute-based neural substrates in temporal cortex for perceiving and knowing about objects. *Nat. Neurosci.* 2, 913.
- Clarke, A., Tyler, L.K., 2014. Object-specific semantic coding in human perirhinal cortex. *J. Neurosci.* 34, 4766–4775.
- Clarke, A., Tyler, L.K., 2015. Understanding what we see: how we derive meaning from vision. *Trends Cognit. Sci.* 19, 677–687.
- Devereux, B.J., Tyler, L.K., Geertzen, J., Randall, B., 2014. The centre for speech, language and the brain (CSLB) concept property norms. *Behav. Res. Methods* 46, 1119–1127.
- De Deyne, S., Storms, G., 2008. Word associations: norms for 1,424 Dutch words in a continuous task. *Behav. Res. Methods* 40, 198–205.
- De Deyne, S., Verheyen, S., Ameer, E., Vanpaemel, W., Dry, M.J., Voorspoels, W., Storms, G., 2008. Exemplar by feature applicability matrices and other Dutch normative data for semantic concepts. *Behav. Res. Methods* 40, 1030–1048.
- De Deyne, S., Navarro, D.J., Storms, G., 2013. Better explanations of lexical and semantic cognition using networks derived from continued rather than single-word associations. *Behav. Res. Methods* 45, 480–498.
- De Deyne, S., Navarro, D.J., Perfors, A., Storms, G., 2016. Structure at every scale: a semantic network account of the similarities between unrelated concepts. *J. Exp. Psychol. Gen.* 145, 1228–1254.
- De Deyne, S., Navarro, D.J., Perfors, A., Brysbaert, M., Storms, G., 2018. The Small World of Words English word association norms for over 12,000 cue words. *Behav. Res. Methods* 1–20.
- Fairhall, S.L., Caramazza, A., 2013. Brain regions that represent amodal conceptual knowledge. *J. Neurosci.* 33, 10552–10558.
- Fan, L., Li, H., Zhuo, J., Zhang, Y., Wang, J., Chen, L., Yang, Z., Chu, C., Xie, S., Laird, A.R., Fox, P.T., Eickhoff, S.B., Yu, C., Jiang, T., 2016. The human brainnetome atlas: a new brain atlas based on connective architecture. *Cerebr. Cortex* 26, 3508–3526.
- Farah, M.J., McClelland, J.L., 1991. A computational model of semantic memory impairment: modality specificity and emergent category specificity. *J. Exp. Psychol. Gen.* 120, 339–357.
- Fernandino, L., Binder, J.R., Desai, R.H., Pendl, S.L., Humphries, C.J., Gross, W.L., Conant, L.L., Seidenberg, M.S., 2015a. Concept representation reflects multimodal abstraction: a framework for embodied semantics. *Cerebr. Cortex* 1–17.
- Fernandino, L., Humphries, C.J., Seidenberg, M.S., Gross, W.L., Conant, L.L., Binder, J.R., 2015b. Predicting brain activation patterns associated with individual lexical concepts based on five sensory-motor attributes. *Neuropsychologia* 76, 17–26.
- Fernandino, L., Humphries, C.J., Conant, L.L., Seidenberg, M.S., Binder, J.R., 2016. Heteromodal cortical areas encode sensory-motor features of word meaning. *J. Neurosci.* 36, 9763–9769.
- Friston, K.J., Holmes, A.P., Worsley, K.J., Poline, J.P., Frith, C.D., Frackowiak, R.S.J., 1995. Statistical parametric maps in functional imaging: a general linear approach. *Hum. Brain Mapp.* 2, 189–210.
- Gainotti, G., 2000. What the locus of brain lesion tells us about the nature of the cognitive defect underlying category-specific disorders: a review. *Cortex* 36, 539–559.
- Gorno-Tempini, M., Hillis, A., Weintraub, S., Kertesz, A., Mendez, M., Cappa, S., Ogar, J., Rohrer, J., Black, S., Boeve, B., Manes, F., Dronkers, N., Vandenberghe, R., Rascovsky, K., Patterson, K., Miller, B., Knopman, D., Hodges, J., Mesulam, M., Grossman, M., 2011. Classification of primary progressive aphasia and its variants. *Neurology* 76, 1006–1014.
- Heeringa, W., 2004. Groningen Dissertations in Linguistics. Measuring Dialect Pronunciation Differences using Levenshtein distance, vol. 46, p. 315.
- Hirabayashi, T., Takeuchi, D., Tamura, K., Miyashita, Y., 2013. Microcircuits for hierarchical elaboration of object coding across primate temporal areas. *Science* 341, 191–195.
- Humphreys, G.W., Forde, E.M., 2001. Hierarchies, similarity, and interactivity in object recognition: "category-specific" neuropsychological deficits. *Behav. Brain Sci.* 24, 453–476.
- Huth, A.G., Heer, W.A.D., Griffiths, T.L., Theunissen, F.E., Jack, L., 2016. Natural speech reveals the semantic maps that tile human cerebral cortex. *Nature* 532, 453–458.
- Jobard, G., Crivello, F., Tzourio-Mazoyer, N., 2003. Evaluation of the dual route theory of reading: a metanalysis of 35 neuroimaging studies. *Neuroimage* 20, 693–712.
- Kivisaari, S.L., Tyler, L.K., Monsch, A.U., Taylor, K.I., 2012. Medial perirhinal cortex disambiguates confusable objects. *Brain* 135, 3757–3769.
- Kivisaari, S.L., Probst, A., Taylor, K.I., 2013. The perirhinal, entorhinal, and parahippocampal cortices and Hippocampus: an overview of functional anatomy and protocol for their segmentation. In: *MR Images in fMRI*. Springer Berlin Heidelberg, Berlin, Heidelberg, pp. 239–267.
- Lambon-Ralph, M.A., Jefferies, E., Patterson, K., Rogers, T.T., 2016. The neural and computational bases of semantic cognition. *Nat. Rev. Neurosci.* 18, 1–14.
- Levenshtein, V., 1966. Binary codes capable of correcting deletions, insertions, and reversals. *Sov. Phys. Dokl.* 10, 707–710.
- Liu, H., Agam, Y., Madsen, J.R., Kreiman, G., 2009. Timing, timing, timing: fast decoding of object information from intracranial field potentials in human visual cortex. *Neuron* 62, 281–290.
- Liuzzi, A.G., Bruffaerts, R., Dupont, P., Adamczuk, K., Peeters, R., De Deyne, S., Storms, G., Vandenberghe, R., 2015. Left perirhinal cortex codes for similarity in meaning between written words: comparison with auditory word input. *Neuropsychologia* 1–13.
- Liuzzi, A.G., Bruffaerts, R., Peeters, R., Adamczuk, K., Keuleers, E., De Deyne, S., Storms, G., Dupont, P., Vandenberghe, R., 2017. Cross-modal representation of spoken and written word meaning in left pars triangularis. *Neuroimage* 150, 292–307.
- Martin, A., 2007. The representation of object concepts in the brain. *Annu. Rev. Psychol.* 58, 25–45.
- Martin, C.B., Douglas, D., Newsome, R.N., Man, L.L., Barense, M., 2018. Integrative and distinctive coding of visual and conceptual object features in the ventral visual stream. *eLife* 7, e31873.
- McRae, K., Cree, G.S., Seidenberg, M.S., McNorgan, C., 2005. Semantic feature production norms for a large set of living and nonliving things. *Behav. Res. Methods* 37, 547–559.
- Mion, M., Patterson, K., Acosta-Cabrero, J., Pengas, G., Izquierdo-Garcia, D., Hong, Y.T., Fryer, T.D., Williams, G.B., Hodges, J.R., Nestor, P.J., 2010. What the left and right anterior fusiform gyri tell us about semantic memory. *Brain* 133, 3256–3268.
- Naya, Y., Yoshida, M., Miyashita, Y., 2001. Backward spreading of memory-retrieval signal in the primate temporal cortex. *Science* 291, 661–664.
- Naya, Y., Yoshida, M., Miyashita, Y., 2003. Forward processing of long-term associative memory in monkey inferotemporal cortex. *J. Neurosci.* 23, 2861–2871.
- Noonan, K.A., Jefferies, E., Visser, M., Lambon Ralph, M.A., 2013. Going beyond inferior prefrontal involvement in semantic control: evidence for the additional contribution of dorsal angular gyrus and posterior middle temporal cortex. *J. Cognit. Neurosci.* 25, 1824–1850.
- Peelen, M.V., Caramazza, A., 2012. Conceptual object representations in human anterior temporal cortex. *J. Neurosci.* 32, 15728–15736.
- Poline, J.B., Worsley, K.J., Evans, A.C., Friston, K.J., 1997. Combining spatial extent and peak intensity to test for activations in functional imaging. *Neuroimage* 5, 83–96.
- Price, A.R., Bonner, M.F., Peelle, J.E., Grossman, M., 2017. Neural coding of fine-grained object knowledge in perirhinal cortex. *bioRxiv* 1–18, 194829.

- Quiroga, R.Q., Reddy, L., Kreiman, G., Koch, C., Fried, I., 2005. Invariant visual representation by single neurons in the human brain. *Nature* 435, 1102–1107.
- Ranganath, C., Ritchey, M., 2012. Two cortical systems for memory-guided behaviour. *Nat. Rev. Neurosci.* 13, 713–726.
- Ritchey, M., Montchal, M.E., Yonelinas, A.P., Ranganath, C., 2015. Delay-dependent contributions of medial temporal lobe regions to episodic memory retrieval. *eLife* 1–19, 2015.
- Sakai, K., Miyashita, Y., 1991. Neural organization for the long-term memory of paired associates. *Nature* 354, 152–155.
- Shaywitz, S.E., Shaywitz, B.A., 2008. Paying attention to reading: the neurobiology of reading and dyslexia. *Dev. Psychopathol.* 20, 1329–1349.
- Tyler, L.K., Stamatakis, E.A., Bright, P., Acres, K., Abdallah, S., Rodd, J.M., Moss, H.E., 2004. Processing objects at different levels of specificity. *J. Cognit. Neurosci.* 16, 351–362.
- Tyler, L.K., Chiu, S., Zhuang, J., Randall, B., Devereux, B.J., Wright, P., Clarke, A., Taylor, K.I., 2013. Objects and categories: feature statistics and object processing in the ventral stream. *J. Cognit. Neurosci.* 25, 1723–1735.
- Vandenbulcke, M., Peeters, R., Fannes, K., Vandenberghe, R., 2006. Knowledge of visual attributes in the right hemisphere. *Nat. Neurosci.* 9, 964–970.
- Wandell, B.A., Rauschecker, A.M., Yeatman, J.D., 2010. Learning to see words. *Annu. Rev. Psychol.* 31–53.